Environmental Pollution 264 (2020) 114585

Contents lists available at ScienceDirect

Environmental Pollution

journal homepage: www.elsevier.com/locate/envpol

Role of the proteome in providing phenotypic stability in control and ectomycorrhizal poplar plants exposed to chronic mild Pb stress☆

Agnieszka Szuba [a, *], Łukasz Marczak [b], Rafał Kozłowski [c]

[a] Institute of Dendrology, Polish Academy of Sciences, Parkowa 5, 62-035, Kórnik, Poland
[b] Institute of Bioorganic Chemistry, Polish Academy of Sciences, Noskowskiego 12/14, 61-704, Poznań, Poland
[c] Institute of Geography and Environmental Sciences, Jan Kochanowski University, Universytecka 7, 24-406, Kielce, Poland

ARTICLE INFO

Article history:
Received 31 December 2019
Received in revised form
9 March 2020
Accepted 9 April 2020
Available online 15 April 2020

Keywords:
Root proteome
Root metabolome
Heavy metals
Ectomycorrhiza
Increased tolerance

ABSTRACT

Lead is a dangerous pollutant that accumulates in plant tissues and causes serious damage to plant cell macromolecules. However, plants have evolved numerous tolerance mechanisms, including ectomycorrhizae, to maintain cellular Pb^{2+} at the lowest possible level. When those mechanisms are successful, Pb-exposed plants should exhibit no negative phenotypic changes. However, actual molecular-level plant adjustments at Pb concentrations below the toxicity threshold are largely unknown, similar to the molecular effects of protective ectomycorrhizal root colonization. In this study, we (1) determined the molecular adjustments in plants exposed to Pb but without visible Pb stress symptoms and (2) examined ectomycorrhizal root colonization (the role of fungal biofilters) with respect to molecular-level Pb perception by plant root cells. Biochemical, microscopic, proteomic and metabolomic studies were performed to determine the molecular status of *Populus* × *canescens* microcuttings grown in agar medium enriched with 0.75 mM $Pb(NO_3)_2$. Noninoculated and inoculated with *Paxillus involutus* poplars were analyzed in two independent comparisons of the corresponding control and Pb treatments. After six weeks of growth, Pb caused no negative phenotypic effects. No Pb-exposed poplar showed impaired growth or decreased leaf pigmentation. Proteomic signals of intensified Pb sequestration in the plant cell wall and vacuoles, cytoskeleton modifications, H^+-ATPase-14-3-3 interactions, and stabilization of protein turnover in chronically Pb-exposed plants co-occurred with high metabolomic stability. There were no differentially abundant root primary metabolites; only a few differentially abundant root secondary metabolites and no Pb-triggered ROS burst were observed. Our results strongly suggest that proteome adjustments targeting Pb sequestration and ROS scavenging, which are considerably similar but less intensive in ectomycorrhizal poplars than in control poplars due to the *P. involutus* biofilter (as confirmed in a mineral study), were responsible for the metabolomic and phenotypic stability of poplars exposed to chronic mild Pb stress.

1. Introduction

Lead is one of the most dangerous nonessential heavy metals for living organisms. In stressed plants, Pb causes DNA mutations, lipid peroxidation or improper folding and aggregation of proteins. As a result, Pb disrupts key metabolic processes in plant cells and inhibits plant growth (Michalak, 2006; Jiang et al., 2018; Fahr et al., 2013; Luo et al., 2014; Hasan et al., 2017; Zhang et al., 2017a).

However, plants have developed numerous defensive mechanisms of which the common denominator is that they decrease the free Pb^{2+} concentration in the plant cell cytosol. The mechanisms of heavy metal (HM) detoxification involve HM retention in the rhizosphere that is triggered by exudation of various organic ligands (Shahid et al., 2012; Reddy et al., 2016). Pb is also chelated in the plant cell wall (CW) by cellulose, hemicellulose, lignin, callose and pectin (Williams et al., 2000; Krzesłowska, 2011). When the CW is overloaded, Pb^{2+} ions are transported via the plasma membrane (PM) by various, usually ATP-related, metal transporters. P-type ATPases and PPi-ATPases play important roles in providing the necessary driving force for this transport (Klychnikov

☆ This paper has been recommended for acceptance by Jörg Rinklebe.

* Corresponding author.
E-mail address: aszuba@man.poznan.pl (A. Szuba).

https://doi.org/10.1016/j.envpol.2020.114585

et al., 2007). Once Pb ion enters the symplast, it is bound in various chelates and then redirected to the vacuole, the main and final site of Pb sequestration in plant protoplasts (Sharma et al., 2016; Hasan et al., 2017). When Pb sequestration processes are inefficient, Pb^{2+} in the cytosol triggers a burst of reactive oxygen species (ROS) (Jalmi et al., 2018). To avoid negative effects of ROS on macromolecules in Pb-stressed plants, enzymatic (peroxidases, catalase, superoxide dismutase) or nonenzymatic (e.g., glutathione) antioxidants are activated (Pourrut et al., 2013; Hasan et al., 2017). Proteins are protected by massively overproduced heat shock proteins (HSPs) (Hasan et al., 2017; Wang et al., 2004).

All the mentioned mechanisms were recognized in the considerable majority of plants that exhibit Pb stress symptoms. However, lead has a strong potential to precipitate with many anions (Kopittke et al., 2008; Tangahu et al., 2011), and even relatively high total amounts of Pb in soil, when precipitated, may not cause significant changes in plant phenotype (Luo et al., 2014; Szuba et al., 2017; Jiang et al., 2018).

Surprisingly, the plant molecular (omic) response to a Pb dose below the toxicity threshold level has not been determined.

Ectomycorrhizae (ECM) are important players in the alleviation of HM stress (Jentschke and Godbold, 2000; Szuba, 2015; Szuba et al., 2017; Zhang et al., 2017b), their symbiotic association is believed to increase plant HM tolerance (Smith and Read, 2008).

Alleviation of Pb stress by ECM may be may occur by two distinct but usually coexisting mechanisms.

First, improved CO_2 assimilation and nutrient, water, antioxidant and carbohydrate status directly increases mycorrhizal plant biomass, vitality and host resistance to subsequent HM stress (Colpaert et al., 2011; Luo et al., 2014; Yamaji et al., 2016; Wang et al., 2018; Shi et al., 2019).

Second, the increased tolerance of ECM plants to Pb is due to the presence of fungal hyphae covering plant root tips and creating mantles (Smith and Read, 2008). In fungal cells, Pb is detoxified and sequestered in a manner very similar to the processes reported in plant cells (Marschner et al., 1998; Jentschke and Godbold, 2000; Johansson et al., 2008; Colpaert et al., 2011; Luo et al., 2014; Shi et al., 2019). Thus, it is believed that fungal hyphae create a biofilter that significantly decreases Pb concentrations in plant cells (Marschner et al., 1998; Jentschke and Godbold, 2000; Wang et al., 2010; Colpaert et al., 2011; Luo et al., 2014; Szuba et al., 2017).

However, fungi release large amounts of low-molecular-weight organic acids (LMWOAs) to fill a key role in symbiosis - increased uptake of essential, poorly soluble nutrients, such as P and Ca (Shahid et al., 2012). For this purpose, large amounts of protons are excluded from the extracellular space. As a result, soil Pb bioavailability is increased (Shahid et al., 2012), and ectomycorrhizal plants are frequently characterized by increased HM uptake (e.g., Zhang, et al., 2017b; Shi et al., 2019). The protective role of the fungal mantle, therefore, may be challenged (Jentschke and Godbold, 2000; Tang et al., 2019).

Because ECM usually increase plant biomass, distinguishing whether the molecular effects triggered by the protective role of ECM are caused by a generally better fitness level of the inoculated plants or by the hyphae biofilter is a challenging task.

In our study, we analyzed *Populus* × *canescens* microcuttings, the growth of which was inhibited by colonization by *Paxillus involutus* (Szuba, unpublished data). Symbiotic partners were grown in excess Pb for six weeks without significant inhibition of plant growth compared to the growth of nonstressed plants. This experimental system provides a unique opportunity to analyze the response of ectomycorrhizal plants to Pb stress influenced by the presence of a biofilter created by fungal hyphae but not by increased plant fitness caused by ECM.

In the present manuscript, an integrated proteomic and metabolomic approach was first used to examine the unknown molecular status of poplars in response to chronic low Pb stress: we planned to assess, from the known Pb stress response mechanisms, the actual key players in the plant response to Pb levels not exceeding the toxicity threshold. Second, we tested the protective role of the fungal mantle biofilter in the Pb stress response of ectomycorrhizal plants.

2. Materials and methods

2.1. Poplar trees and fungal cultures

Freshly transferred *Populus* × *canescens in vitro* microcuttings growing on a two-layer agar medium (Murashige and Skoog (MS) medium covered with modified Melin-Norkrans (MMN) medium) were inoculated as described by Szuba et al. (2017). Barcoded mycelial fragments originating from the poplar monoculture *P. involutus* were used for inoculation. Both inoculated ('M' treatment) and noninoculated ('NM' treatment) plants were grown on control medium ('Control' treatment) or medium supplemented with 0.75 mM $Pb(NO_3)_2$ ('Pb' treatment), resulting in a total of four analyzed treatments (NM-Control, NM-Pb, M-Control and M-Pb; $16 \leq n \leq 19$). Nitrogen was compensated in the Controls with 0.75 mM NH_4NO_3.

Poplar cultures were grown in a growth chamber at 21 °C and 60% relative humidity with a 16-h/8-h day/night photoperiod using cool white fluorescent light (150 μmol m^{-2} s^{-1}). Additionally, for the metabolomic study, a pure culture of *P. involutus* was cultivated in the dark in MMN medium on Petri dishes (Szuba et al., 2017).

2.2. Harvesting and biometric and root colonization analysis

Six weeks after inoculation, the leaves, stems and roots were weighed. Samples of roots, agar medium and *P. involutus* hyphae (from pure culture) were immediately frozen in liquid nitrogen and stored at −80 °C until analysis.

Root tips were divided into three categories, 'nonmycorrhized' root tips and root tips in two stages of colonization. 'Changed' root tips were root tips devoid of root hairs and covered with fungi but lacked a fully developed Hartig net (HN), which is a structure of fungal cells that penetrates the plant root epidermis and cortex to create a network characteristic of functional ECM. The other colonize root tips were swollen, shortened 'fully mycorrhized' root tips with a well-developed mantle and HN. The root tip morphotype percentages were determined using ImageJ 1.48v software (Wayne Rasband) on high-resolution images that were captured during harvest. Categorization was performed based on the anatomical structure of representative root tip morphotypes that were selected during harvest and immediately analyzed under a microscope according to the method reported by Szuba et al. (2017, 2019).

2.3. H_2O_2 detection by confocal laser scanning microscopy (CLSM)

H_2O_2 was visualized in freshly harvested poplar roots by CLSM using a dihydrorhodamine 123 (Sigma Aldrich) probe. Whole roots were incubated for 1 h at 22 °C in the dark (10 μM solutions prepared in 10 mM Tris−HCl, pH 7.4) and examined using a Leica TCS Sp5 equipped with an argon laser. The green fluorescence of oxidized rhodamine 123 (excitation 488 nm; emission 530 nm) was collected simultaneously with bright-field micrographs. The images were collected from three plants per treatment and analyzed using Leica Application Suite X 3.3.0.16799 software. For the CLSM analysis only, an additional acute Pb stress treatment was prepared. Briefly, M-Control and NM-Control roots from 3 plants were incubated in a 0.75 mM $Pb(NO_3)_2$ Milli-Q solution for 2 h and then

immediately used for microscopic study.

2.4. Biochemical analysis

Pooled leaf (100 μg), stem (40 μg) and root (10 μg; whole root systems were used for all, biochemical and omic, analyses) dried samples were used to measure mineral content. Analyses of Pb (and foliar P, K, Mg, Fe, Cu and Zn) were completed using an inductively coupled plasma time-of-flight mass spectrometer (GBC Scientific Equipment). Total nitrogen and carbon were determined in dried leaf samples (3 μg per sample) using a CHNS analyzer (2400 CHNS/O Series II System, PerkinElmer, Waltham, MA).

Leaf pigments were analyzed using pooled samples of fresh leaves immediately after harvest. Chlorophyll *a*, chlorophyll *b* and the sum of xanthophylls and carotenes (total carotenoids) were measured according to the photometric acetone method (Szuba et al., 2017) and normalized to the fresh weight.

2.5. Proteome analysis

Root proteins were isolated from 100 mg of root sample according to the modified phenol extraction method described by Szuba et al. (2019) and resuspended in buffer (4 M urea, 50 mM ammonium carbonate). A minimum of five biological repetitions were performed per treatment.

Root protein extracts (10 μg of protein per run) were digested in standard solution and analyzed by nano-ultraperformance liquid chromatography-tandem mass spectrometry (nano-UPLC-MS/MS) analysis on an OrbiTrap mass spectrometer (Thermo QExactive). Mass spectra were analyzed with MaxQuant 1.5.3.30 (Max Planck) software and compared against the Swiss-Prot database entries using the Viridiplantae taxonomy filter (for details of the mass spectrometry analyses, see File S1).

2.6. Metabolome analysis

2.6.1. LC-MS/MS analysis

Metabolites for liquid chromatography-tandem mass spectrometry (LC-MS/MS) were isolated from 50 mg of root by methanol extraction according to the method reported by Szuba et al. (2013) and immediately analyzed with a Waters Acquity UPLC system connected to a micrOTOF-Q mass spectrometer from Bruker Daltonics. The LC-MS/MS analysis was focused on phenolics, but other compounds characterized by similar polarity, such as phospholipids, were coextracted and detected. Detailed information regarding the MS/MS analysis is presented in File S1. The resultant mass spectra were analyzed using the DataAnalysis version 4 package (Bruker). Fragmentation patterns in the mass spectra were analyzed manually to identify particular compounds (via structural formulas). The integrated chromatographic peaks were used to calculate peak areas of interest.

Glycerophosphocholines (GPCs; recognized based on their fragmentation patterns) were identified by exact mass using the LIPID_MAPS database (www.lipidmaps.org).

2.6.2. GC-MS/MS analysis

Metabolites for gas chromatography-tandem mass spectrometry (GC-MS/MS) were isolated from 5 mg of roots and *P. involutus* mycelium by methanol extraction and further derivatized in a standardized manner (Swarcewicz et al., 2017). The GC-MS/MS experiment was designed to analyze carbohydrates, amino acids and other primary metabolites, but some other compounds, such as phenolics, were also identified. The obtained extracts were separated using an Agilent 7890A gas chromatograph and analyzed with a Pegasus 4D GCxGC-TOFMS mass spectrometer (Leco). Data acquisition, automatic peak detection, mass spectrum deconvolution, retention index calculation and automatic metabolite identification by library (NIST library) searches were performed using LECO ChromaTOF software. For detailed information on the GC-MS/MS experiment and data analysis, see File S1.

2.7. Statistical and bioinformatics analysis

Statistical analyses were performed using JMP Pro 13.0.0 (SAS Institute Inc.) and Perseus (Max Planck) software.

JMP Pro 13.0.0 was used for the statistical analyses of biometric and selected biochemical (e.g., leaf pigments and mineral composition) features of poplars. Values were considered significant at $p < 0.05$ according to the *t*-test for two-sample tests and according to ANOVA/honestly significant difference (HSD) post hoc test for multisample analyses.

Statistical calculations for large molecular datasets (proteomic and metabolomic analysis) were performed using Perseus software. All numeric values were transformed to a logarithmic scale. The missing values were replaced by imputation (File S1). For hierarchical clustering analysis, data were normalized using the Z-score algorithm; only significantly different compounds (according to the *t*-test for two-sample tests and according to ANOVA for multisample tests, FDR = 0.05) are presented.

3. Results

3.1. Biometrics and the root colonization ratio

The inoculated (M) poplars were smaller than the non-inoculated (NM) plants (Fig. 1a and b; see also Fig. S1). There were no differences in poplar height between the corresponding Control and Pb treatments (Fig. 1a), but the mass of M-Pb poplars was greater than that of M-Control plants because of the increased mass of leaves and stems (Fig. 1b, Fig. S1). Pb exposure did not significantly affect the mass of NM poplars (Fig. 1 and b). For both height and fresh weight (FW), an nonsignificant decrease trend for the NM treatment and an nonsignificant increase trend for the M treatment were observed in the presence of Pb (Fig. 1a and b; compared with the corresponding control values).

The total percentage of root tip colonization for both M treatments was approximately 90% and did not differ between the M-Control and M-Pb treatments (Fig. 1c). The clear domination of changed root tips was detected in all colonized plants (Fig. 1c). Similarly, ergosterol (indicator of fungal biomass; not detected in NM roots; Fig. 1d) abundance estimated on the basis of comparison with *P. involutus* hyphae (Fig. 1d) did not differ between the two mycorrhizal treatments, and fungal biomass accounted for less than 4% of the whole root biomass (Fig. 1e).

The Pb concentration was highest in roots of both NM-Pb and M-Pb treatments (Fig. 1f) and it was significantly lower in roots, stems and leaves of M-Pb plants than in those of NM-Pb plants (Fig. 1f). Pb content (per plant) was lower in aboveground tissues of M-Pb poplars than in those of NM-Pb plants (Fig. 1g), whereas it did not differ significantly in roots between NM-Pb and M-Pb treatments (Fig. 1g), which probably occurred because the M-Pb root samples also contained fungal hyphae (characterized by a higher dry mass content and Pb concentration than plant roots; data not shown).

ECM triggered increases in leaf pigments (Table 1) and foliar C and N concentrations and decreases in the concentrations of numerous elements in leaves (Table 1). Pb exposure had different effects on the NM and M foliar mineral composition (Table 1), but no decrease was observed in the majority of metals in either Pb treatment. Leaf pigments were not changed in Pb-exposed poplars compared with the corresponding controls (Table 1).

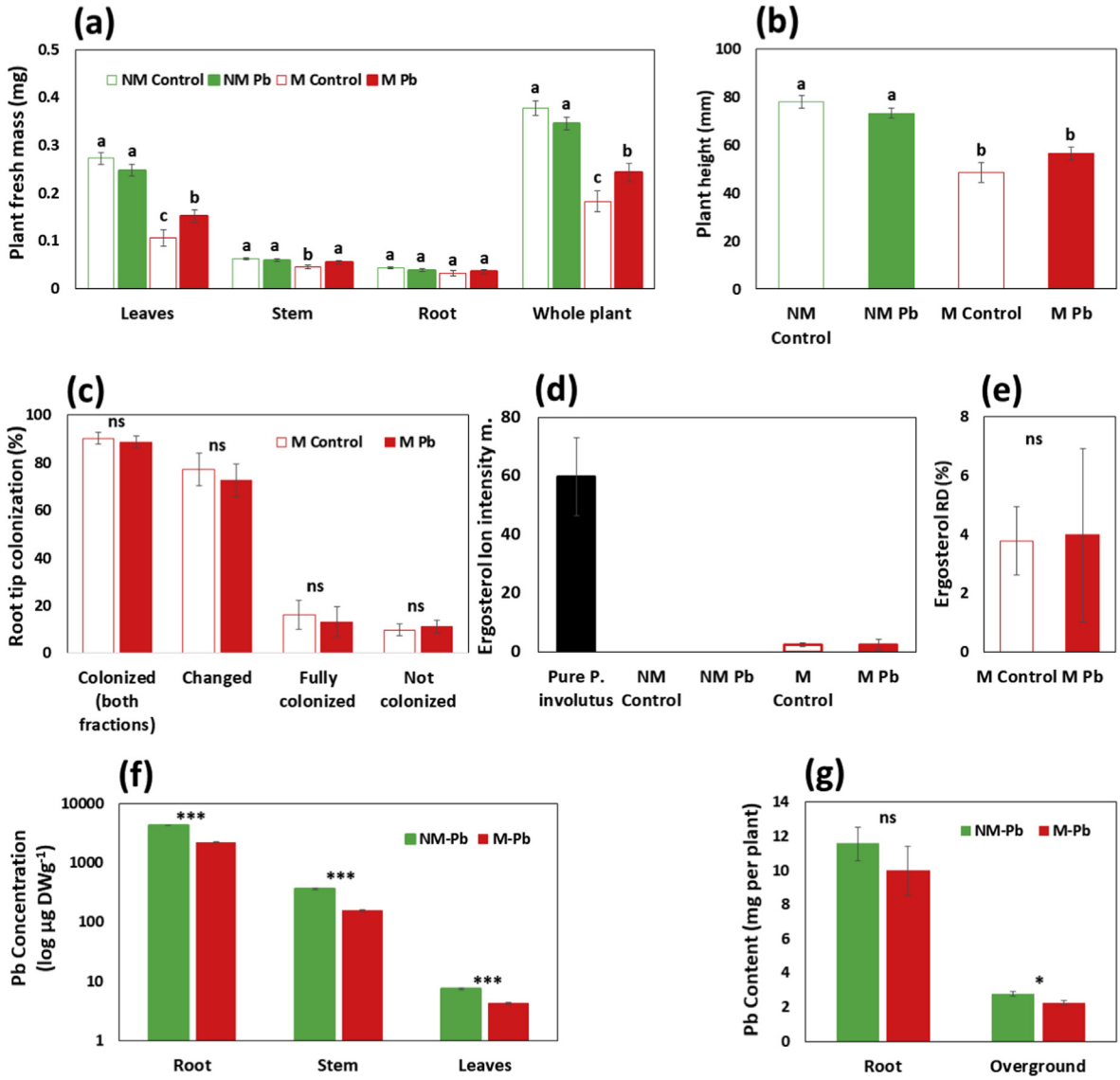

Fig. 1. Biometrics, root colonization and Pb levels. Fresh mass (**a;** n = 13) and height (**b;** n = 13) of the analyzed poplars. Root tip colonization percentage (**c;** n = 13). Ion intensity of ergosterol (**d;** n = 3) and relative percentage of ergosterol ion intensity estimated for mycorrhizal treatments; 100% = ergosterol ion intensity detected in pure culture of *P. involutus* (**e;** n = 3). Pb concentrations (**f**; n = 6) and contents (**g**; n = 13). Mean values ± SEs are presented. Different letters or asterisks (ns = not significant; $*p < 0.05$; $***p < 0.001$) represent significant differences according to the HSD post hoc or *t*-test test.

Table 1
Biochemical characteristics of *Populus* × *canescens* microcuttings. Mean and ±SE values are presented. Significance: *t*-test.

Element	NM Control	NM Pb	M Control	M Pb	Significance			n
					NM vs M	NM vs NM Pb	M vs M Pb	
Foliar elemental composition								
C (g $FWkg^{-1}$)	46.0 ± 0.279	45.0 ± 0.178	113 ± 9.47	125 ± 12.52	<.0001	ns	<.0001	3
N (g $FWkg^{-1}$)	5.05 ± 0.006	4.87 ± 0.021	6.34 ± 0.170	6.00 ± 0.145	<.0001	ns	ns	3
P (mg $FWkg^{-1}$)	548 ± 6.54	580 ± 15.5	562 ± 14.4	695 ± 16.4	ns	ns	<.0001	6
K (mg $FWkg^{-1}$)	4499 ± 100	4740 ± 265	5112 ± 349	5901 ± 203	ns	ns	0.035	6
Mg (mg $FWkg^{-1}$)	292 ± 6.96	287 ± 5.33	230 ± 4.78	293 ± 8.82	<0.001	ns	<0.001	6
Fe (mg $FWkg^{-1}$)	53.0 ± 0.988	123 ± 3.24	19.3 ± 2.07	20.8 ± 4.53	<0.001	<0.001	ns	6
Cu (mg $FWkg^{-1}$)	1.60 ± 0.052	2.15 ± 0.079	0.856 ± 0.055	0.820 ± 0.080	<0.001	<0.001	ns	6
Zn (mg $FWkg^{-1}$)	24.4 ± 0.304	26.8 ± 0.244	21.7 ± 0.331	17.0 ± 0.468	<0.001	<0.001	<0.001	6
Leaf pigments								
Chlorophyll *a* (mg FWg^{-1})	2.41 ± 0.090	2.61 ± 0.045	2.82 ± 0.206	3.15 ± 0.153	0.043	ns	ns	6
Chlorophyll *b* (mg FWg^{-1})	0.616 ± 0.557	0.670 ± 0.017	0.735 ± 0.059	0.794 ± 0.031	0.034	ns	ns	6
Carotenoids (mg FWg^{-1})	0.775 ± 0.026	0.827 ± 0.016	0.931 ± 0.045	0.997 ± 0.033	0.002	ns	ns	6

3.2. Root proteome

3.2.1. NM-Pb vs NM-Control

In NM poplars, 87 proteins were differentially abundant between the NM-Control and NM-Pb treatments (Table S1). Catalase and peroxidase were more abundant in NM-Pb roots (see chapter below), similar to HSP90 and HSP80, but stress-related proteins were generally sparse in Pb-treated NM poplars (Table S1).

Among the less-abundant proteins in the NM-Pb treatment, numerous enzymes involved in transcription (e.g., DEAD-box ATP-dependent RNA helicase), protein biosynthesis (e.g., numerous ribosomal subunits and elongation factors) and folding (e.g., peptidyl-prolyl cis-trans isomerase and HSP70 chaperone) were detected (Fig. 2a and Table S1). Proteins involved in protein degradation, including ubiquitin and both ATP-dependent and ATP-independent 26S proteasome regulatory subunits involved in proteasome functioning, were likewise less-abundant in NM-Pb plants.

In roots, several proteins involved in photosynthesis were found, all of which were less abundant in NM-Pb root cells than in NM-Control root cells (Table S1).

Among the differentially abundant NM proteins, several 14-3-3-like proteins were detected, all of which were less abundant in the Pb treatment. Actin (with the exception of P53492) was less abundant in NM-Pb roots than in NM-Control roots, but tubulin was more abundant in the former (Fig. 2a and Table S1).

Several enzymes involved in N assimilation and metabolism such as glutamine synthetase and sarcosine oxidase were more abundant in NM-Pb roots (Fig. 2a).

The majority of the proteins whose abundances increased in the NM-Pb treatment were associated with carbon metabolism, but only a few glycolytic–TCA cycle enzymes were differentially abundant (Table S1). Among these proteins, those involved in glycolytic bypass, e.g., cytosolic phosphoenolpyruvate carboxylase and malate dehydrogenase, were more abundant in the NM-Pb treatment than in the NM-Control treatment. Additionally, enzymes that metabolize various sugars, such as alpha-mannosidase or sorbitol dehydrogenase, and enzymes involved in noncellulosic CW carbohydrate biosynthesis, e.g., UDP-araginopyranose mutase and UDP-glucose 6-dehydrogenase, were more abundant in NM-Pb roots (Table S1).

One of the most abundant protein groups in NM-Pb root cells consisted of various subunits of V-type proton ATPases, a PM ATPase and ADP. ATP carrier proteins were more abundant in NM roots exposed to Pb stress than in NM-Control roots (Table S1).

Numerous oxidoreductases, alcohol dehydrogenases and aldo-keto reductases were repeatedly detected in greater abundance in NM-Pb root cells than in the NM-Control root cells (Table S1).

3.2.2. M-Pb vs M-Control

Differentially abundant proteins between the M-Control and M-Pb treatments were less numerous than those in noncolonized poplars (23 proteins; Table S1). However, many similarities to the NM root response to Pb^{+2} ions may be found in M plants (Fig. 2a), including eleven proteins that were common to both analyses (differentially abundant between NM-Control and NM-Pb treatments and between M-Control and M-Pb treatments; Fig. 2b). According to a hierarchical clustering analysis, the ion intensities of 'common proteins' were highly similar under Pb stress regardless of *P. involutus* colonization (Fig. 2b). All the common proteins showed a similar response between the corresponding Control and Pb

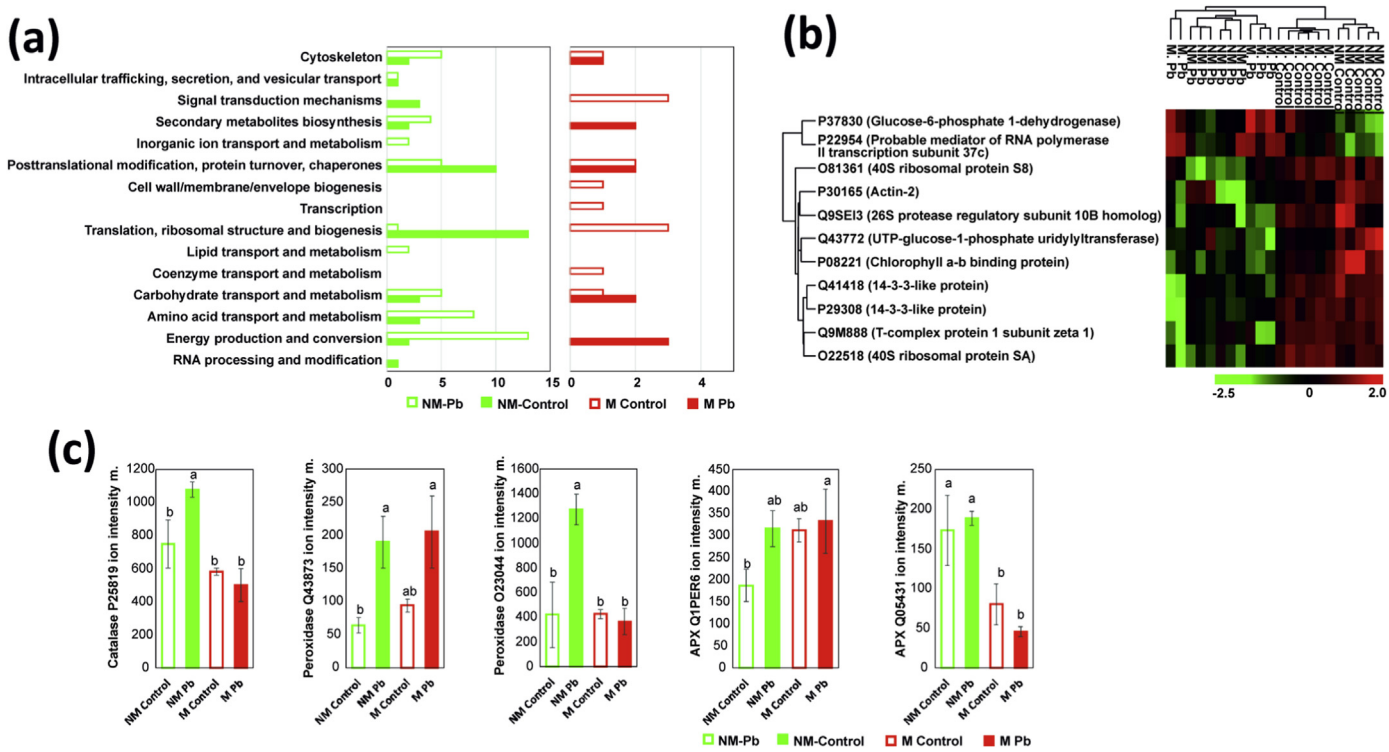

Fig. 2. Protein data. Graphical presentation of the differentially abundant clusters of orthologous groups (COG) protein classes between the analyzed treatments according to both two-sample t-tests (NM-Control vs NM-Pb and M-Control vs M-Pb) (**a**). The number of proteins representing individual groups is given. Common proteins (**b**). Heat map analysis combined with hierarchical cluster analysis showing differentially abundant poplar root proteins ($p < 0.05$) according to both two-sample tests (NM-Control vs NM-Pb and M-Control vs M-Pb). Green, minimal abundance; red, maximal abundance. Abundance of antioxidative root enzymes (**c**). Nontransformed ion intensities of all antioxidative enzymes detected as differently abundant (according to multisample ANOVA test) were analyzed using JMP Pro 13.0.0 software. Mean values ± SEs are presented. Different letters indicate significant differences according to the HSD post hoc test. (For interpretation of the references to colour in this figure legend, the reader is referred to the Web version of this article.)

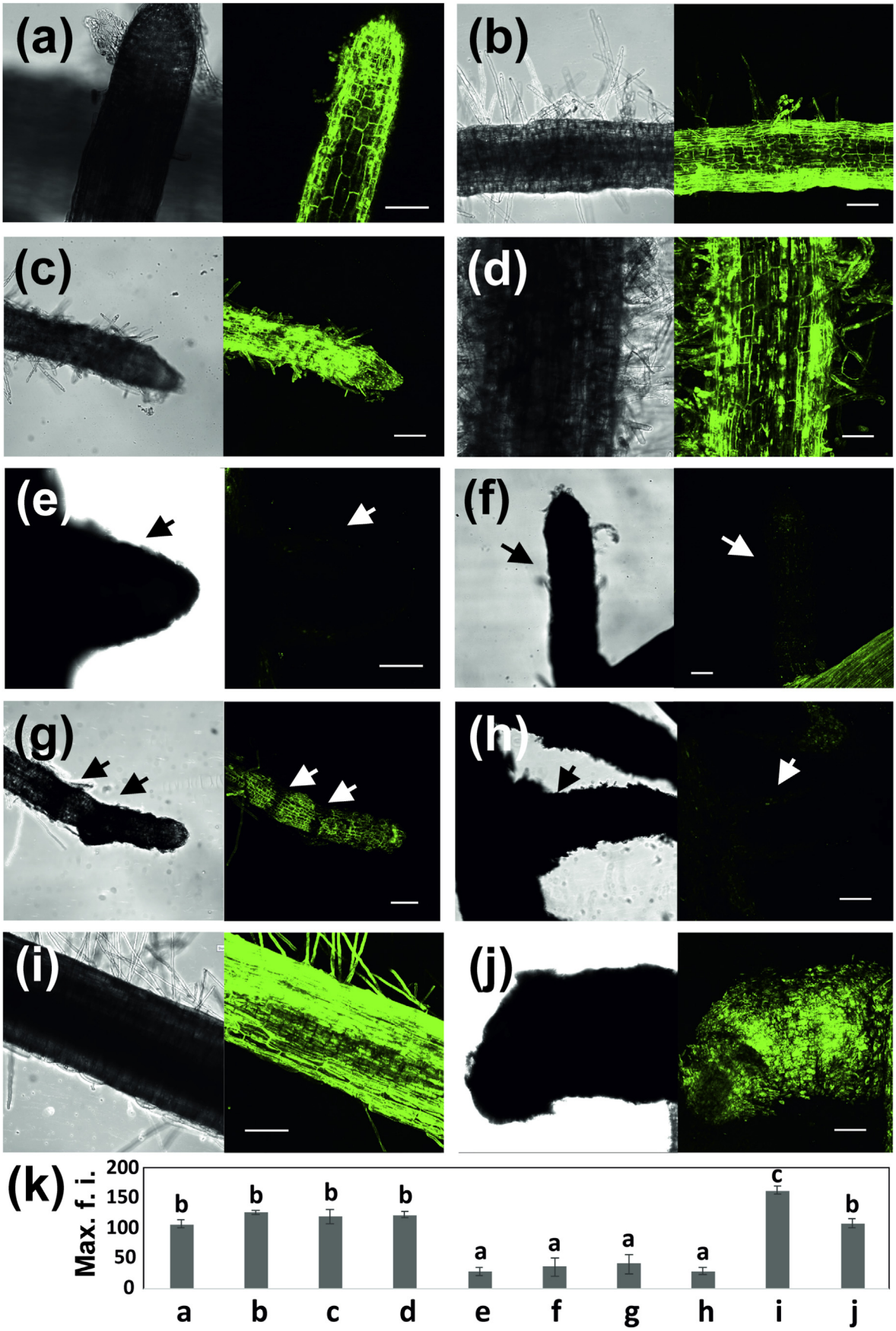
(a)
(b)
(c)
(d)
(e)
(f)
(g)
(h)
(i)
(j)
(k)
Max. f. i.
200
150
100
50
0
b
b
b
b
a
a
a
a
c
b
a
b
c
d
e
f
g
h
i
j

treatments, and the expression of a majority of them was down-regulated in all plants exposed to Pb^{2+} ions (Fig. 2b). A reduced abundance in the M-Pb treatment was observed for ribosomal proteins, the proteasome subunit involved in ATP-dependent protein degradation, 14-3-3-like proteins, actin, the T-complex protein subunit (an ATP-dependent chaperone involved in actin and tubulin polymerization) and UTP-glucose-1-phosphate uridylyltransferase.

A glycolytic enzyme (here enolase) and glucose-6-phosphate 1-dehydrogenase, involved in the pentose-phosphate pathway, were more abundant in M-Pb roots than in M-Control roots, similar to the pattern in NM plants. The subunit of vacuolar V-type proton ATPase showed a higher abundance in M-Pb plants (Table S1).

In contrast to the case in NM poplars, most photosynthesis-related enzymes were more abundant in M-Pb roots than in M-Control roots, with the exception of chlorophyll *a-b* binding protein (Table S1).

Among the proteins whose abundances increased in response to M-Pb treatment, no HSPs, antioxidative enzymes or other enzymes directly related to the stress response were detected.

All these changes were reflected in the clusters of orthologous groups (COG) classification (Fig. 2a; for detailed data on protein identification, please see Table S1).

3.3. Anti-ROS root enzymes and H_2O_2 abundance

According to a proteome analysis comparing NM and M treatments, only one ascorbate peroxidase (APX) protein was differentially abundant and exhibited decreased abundance in ectomycorrhizal poplars (among proteins selected during ANOVA multisample test; Fig. 2c). Compared with the NM-Control root enzymes, all identified anti-ROS enzymes tended to be more abundant in NM-Pb roots, but a significant difference was found for only peroxisomal catalase and two apoplastic peroxidases. No clear trends in abundance and no anti-ROS enzymes significantly differed in abundance in M-Pb vs M-Control treatments (Fig. 2c).

The distribution of ROS on Pb-treated roots was observed using CLSM. As an ROS example, H_2O_2 was indicated on the basis of differently abundant anti-ROS enzymes that play a key role in H_2O_2 detoxification, i.e., catalase and peroxidases. Representative images of the analyzed treatments are shown in Fig. 3a–j, and the quantified data on H_2O_2 generation are shown in Fig. 3k. Compared to that in NM treatments (Fig. 3a and b), H_2O_2 was less abundant in mycorrhizal plants (Fig. 3e and f) in both apical (tip) and root hair zones (Fig. 3k). Fluorescence decreased or was even undetectable in M treatments, especially in root fragments covered with fungal cells (mantles; Fig. 3e and f (arrows)). No significant differences were found in fluorochrome fluorescence intensity between the Pb treatment and the corresponding Control treatment (Fig. 3k). However, when acute Pb^{2+} stress was applied (Fig. 3i and j), the fluorescence increased compared with that in the Control and chronic Pb treatments (Fig. 3k), including strong fluorescence in the hyphae-covered M root tips (Fig. 3j), confirming that H_2O_2 was produced under acute Pb stress and could also be detected in fungal hyphae.

3.4. Root metabolome

3.4.1. GC-MS/MS analysis

Among 282 metabolites identified during GC-MS/MS analysis, 42 were differentially abundant between the analyzed treatments, of which 12 were identified by formula (Fig. 4a). Carbohydrates, organic acids, phenolic compounds and amino acids were differentially abundant in our study (Fig. 4a). However, no differences were found between the NM-Control and NM-Pb treatments or between the M-Control and M-Pb treatments (Fig. 4a).

3.4.2. LC-MS/MS analysis

Among the detected root compounds in the LC-MS/MS analysis, only a few were differentially abundant between the corresponding Control and Pb treatments (fewer than 1% of detected compounds; Fig. 4b and c). After a manual spectrum search, most detected metabolites remained unknown; however, several compounds were identified by formula, such as GPCs and phenolic compounds (Table S2). All the identified GPCs and the majority of phenolic compounds were more abundant in colonized roots than in NM roots (Table S2). The abundance of most of the identified compounds did not differ between the NM-Control and NM-Pb treatments (Table S2). However, almost all GPCs were less abundant in M-Pb roots than in the M-Control roots, whereas almost all phenolics were more abundant in M-Pb poplars than in M-Control plants (Table S2).

4. Discussion

4.1. Molecular status of poplars exposed to Pb but not exhibiting significant negative phenotypic changes

In MS medium, which is rich in phosphates and sulfates, numerous Pb^{2+} ions are likely to be precipitated (Kopittke et al., 2008; Szuba et al., 2017). Nevertheless, Pb was detected in poplar tissues. Simultaneously, no significant negative phenotypic changes characteristic of Pb stress were found in NM-Pb poplars. No decreased plant growth or biomass, leaf chlorosis or impaired nutrient flow were detected in Pb-exposed plants (Fahr et al., 2013; Hasan et al., 2017). Taken together, these results suggest that the Pb toxicity threshold was not exceeded in the analyzed poplars regardless of root colonization (Shi et al., 2019).

4.1.1. Proteomic signals of Pb sequestration in the apoplast

The increased abundance of enzymes involved in the biosynthesis of noncellular carbohydrates in NM-Pb poplars suggested that the plant CW was modulated to increase the number of Pb binding sites. This phenomenon confirms the important role of the plant apoplast during the initial steps of Pb sequestration (Fig. 5a; Krzesłowska, 2011; Luo et al., 2014; Kosová et al., 2015; Li et al., 2016; Shi et al., 2019). Interestingly, we observed strong signals indicative of an increased abundance of tubulin, a cytoskeletal protein involved in chromosome functioning and plant cell division that is a target of even low Pb concentrations (similarly as actin, which was down-regulated in both Pb treatments; Pourrut et al., 2013; Horiunova et al., 2016). The increased tubulin abundance is

Fig. 3. Representative confocal laser scanning microscopy images of NM and M poplar roots showing H_2O_2 abundance as determined by staining with dihydrorhodamine 123. (**a**) Apical (tip) zone of NM-Control treatments. (**b**) Root hair zone of NM-Control treatment. (**c**) Apical zone of NM-Pb treatment (the zone corresponding to the image shown at point a). (**d**) Root hair zone of NM-Pb treatment. (**e**) Apical zone of the M-Control treatment. (**f**) Fragments of roots of M-Control treatment corresponding to the root hair zone, covered with fungal hyphae (marked by an arrow). (**g**) Root apical zone of the M-Pb treatment (covered with fungal hyphae marked by arrows). (**h**) Fragments of roots in the M-Pb treatment corresponding to the root hair zone covered with fungal hyphae (marked by arrows). (**i**) NM-Control root subjected to acute Pb stress (incubated for 2 h in 0.75 mM $Pb(NO_3)_2$ solution). (**j**) M-Control root fully covered by fungal mantle subjected to acute 0.75 mM $Pb(NO_3)_2$ stress. Fluorescence distributions and images under white light (3D images obtained by overlapping multiple optical sections) are presented. Bars: 100 μm. Semiquantification of fluorescence signal intensities in (a–j) (**k**). Mean values ± SEs are presented. Different letters represent significant differences according to the HSD post hoc test (Max. f. i. – Maximum fluorescence intensity).

therefore exceptional. It is possible, however, that we detected increased amounts of cortical tubules. Cortical tubules are known targets of Pb but are also crucial for CW remodeling (for cellulose synthase positioning; Horiunova et al., 2016); in this context, an increased abundance of tubulin could be related to the intensified release of various CW carbohydrates in response to Pb (Fig. 5a).

4.1.2. Pb uptake and further sequestration – possible H+-ATPase and 14-3-3 protein interaction

In NM-Pb poplars, we detected a greater abundance of H^+ATPases, both PM- and V- type, the key players in plant functions (including the HM stress response; Williams et al., 2000; Klychnikov et al., 2007; Colpaert et al., 2011; Shahid et al., 2012; Chen et al., 2015; Liu et al., 2017; Zhang et al., 2017 and 2017b). The proton gradient created by H^+-ATPases may be consumed by, inter alia, various metal transporters involved in Pb uptake (Hasan et al., 2017; Liu et al., 2017) but also by the symport of various organic acids that are responsible for HM sequestration in the rhizosphere (Zhang et al., 2017). V H^+ATPases, which are responsible for tonoplast transport, were more abundant in NM-Pb roots (and more numerous compared with PM H^+ATPases). Rapid Pb efflux from the cytoplasm into the vacuole is crucial for HM cellular homeostasis and tolerance (Zhang et al., 2017 and 2017a). According to our proteomic results, these processes also occurred extensively below the Pb toxicity threshold (Fig. 5a; Sharma et al., 2016).

All H+-ATPases are strictly regulated proton pumps. Changes in ATPase abundance, influencing the sequestration of HMs, are considered long-term regulation processes, whereas short-term regulation of the activity of proton pumps (as well as metal transporters; Hasan et al., 2017; Zhang et al., 2017 and 2017b) is believed to occur via, inter alia, phosphorylation/dephosphorylation processes, and is linked to 14-3-3 protein activity (Wang et al., 2002; Klychnikov et al., 2007; Chen et al., 2015).

Interactions between ATPases and 14-3-3, which are ubiquitous, conserved enzymes regulating the activity of various proteins that are important in stress adaptation (Wang et al., 2002), influence plant HM tolerance (Chen et al., 2015; Xie et al., 2017). The 14-3-3 proteins may bind to phosphorylated motifs in target enzymes and have phosphorylation-dependent interactions with an A-catalytic subunit of ATPases (Wang et al., 2002; Klychnikov et al., 2007; Chen et al., 2015). Both A-catalytic subunits of ATPases and 14-3-3-like protein abundances were significantly modified in Pb-exposed poplar roots.

It has been reported that the abundance and activity of 14-3-3 proteins are increased under various abiotic stress conditions (Chen et al., 2015; Kosová et al., 2015; Zhang et al., 2017) and correlate with HM exposure (in ECM fungi; Xie et al., 2017). In our study, 14-3-3 abundance was significantly decreased, in contrast to the increased H+-ATPase abundance (Fig. 5a). The decrease in 14-3-3 abundance might lead to a decrease in already present transmembrane proton pump activity (according to the current plant root needs; Klychnikov et al., 2007). Such a speculative hypothesis raises the question of why the abundance of 14-3-3 but not that of H+-ATPases was decreased. The increased abundance of proton pumps was necessary for proper Pb sequestration, explaining the increased abundance; however, H+-ATPase activity that is too high may lead to extensive ground medium acidification (not observed for NM-Pb treatment; data not shown) and, consequently, potentially harmful increases in Pb bioavailability. The mechanism allowing the coexistence of an increased abundance of H+-ATPases and strict regulation of their current activity would likely be highly advantageous for long-term plant cell Pb-pH homeostasis. We speculated that in chronically stressed plant cells, it would be less costly to moderate the amount of 14-3-3 than the abundance of ATPase, which is strictly controlled and extremely energy-consuming in its turnover (Babst, 2014; Li et al., 2017) as a transmembrane protein.

All the described Pb-handling mechanisms aim to decrease the free Pb^{2+} level in the cytoplasm. Indeed, in all Pb treatments, we did not detect signals for the activation of chelating compounds that prevent free metal ion circulation in the cytosol (Pourrut et al., 2013; Wang et al., 2013; Hasan et al., 2017), suggesting successful Pb^{2+} ion sequestration (Fig. 5a).

4.1.3. Oxidative stress: scavenging enzymes vs radicals

Oxidative stress and anti-ROS activation are the most frequently reported results of HM exposure (Pourrut et al., 2013; Li et al., 2016; Wang et al., 2016; Zemleduch-Barylska and Lorenc-Plucińska, 2016; Xu et al., 2017). An increased abundance of enzymatic ROS scavengers (and thus, their assumed activity) was also found in our study, confirming the presence of Pb in plant roots.

Most of the upregulated anti-ROS enzymes in NM-Pb roots were apoplastic peroxidases (Fig. 5b); thus, before exceeding the Pb toxicity threshold, the majority of Pb-induced ROS was sequestered and scavenged in the CW area. Indeed, most H_2O_2 was present in the CW area (Fig. 3), making the poplar apoplast the main battlefield with eventual Pb-induced ROS.

Our results suggested, however, that some free Pb^{2+} ions in NM-Pb plants were probably present in the protoplast. According to the proteome analysis, in chronically stressed poplars, the main cytoplasmic enzymes involved in the oxidative stress response triggered by Pb^{2+} were oxidoreductases (aldo-keto reductases and alcohol dehydrogenases; Fig. 5b). These enzymes scavenge reactive cytotoxic carbonyl compounds created during oxidative stress, e.g., peroxidized lipids (Éva et al., 2014; Kirankumar et al., 2016; Vemanna et al., 2017). Our results suggested that such organic radicals were mainly created in the cytosol of NM-Pb plants. Aldo-keto reductases have been shown to protect enzymes against HM-triggered oxidative stress (Éva et al., 2014; Kirankumar et al., 2016; Vemanna et al., 2017).

Activation of the enzymatic anti-ROS response seems to be sufficient to scavenge radicals whose generation was triggered by Pb. In contrast to reported data on Pb-stressed plants (e.g., Wang, et al., 2013), we did not detect (in either Pb treatment) an increased abundance of ROS (Fig. 5), and plants did not exhibit negative phenotypic signals of Pb exposure. The protective role of the enzymatic anti-ROS response, resulting in a low abundance of cytosolic ROS, might also be confirmed by the low abundance of HSPs found in NM-Pb roots and consequent reduced number of misfolded proteins (Wang et al., 2004; Visioli et al., 2012).

4.1.4. Decreased protein biosynthesis and turnover in chronically stressed poplars

One of the most interesting effects of chronic Pb exposure on poplar roots was decreased protein turnover (Fig. 5a). HM stress usually triggers a strong transcriptomic response (Shen et al., 2013; Wang et al., 2013; Luo et al., 2014; Jalmi et al., 2018; Zhang et al., 2017a), which translates to an upregulation of stress-related protein expression (Pourrut et al., 2013; Li et al., 2016), including elements of the translational machinery itself (Moin et al., 2017), which is opposite to the findings in the present study. Because one of the major results of HM exposure is protein damage, a massive upregulation of HSP70 expression is one of the most frequently observed effects of Pb on the plant proteome (Kosová et al., 2015; Wang et al., 2004). Similarly, damaged and aggregated proteins usually undergo constant degradation (e.g., Hasan, et al., 2017). In this context, our proteomic results, clearly suggesting a decrease in all the mentioned processes of protein turnover in Pb-exposed poplars, are rather surprising.

The explanation may be related to the stress dose and duration.

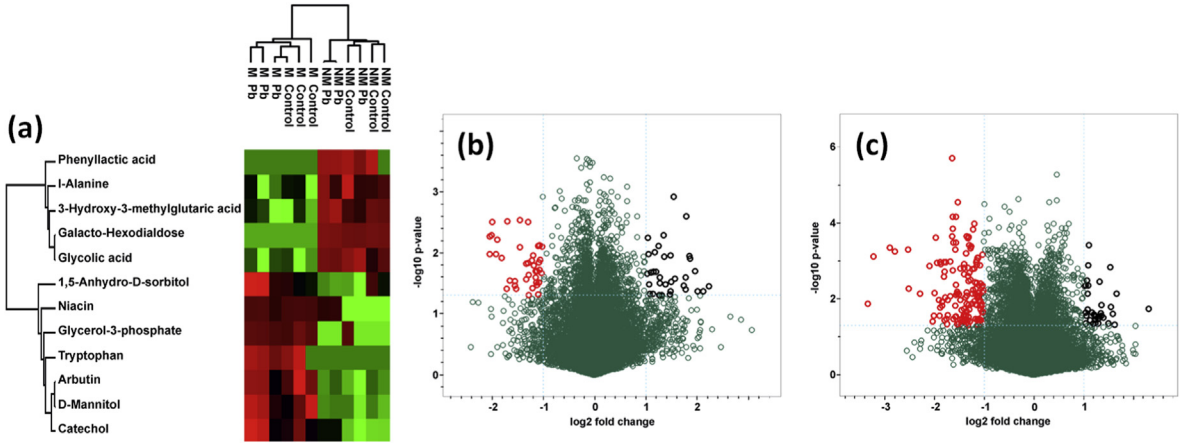

Fig. 4. Metabolomic analysis. Heat map analysis combined with hierarchical cluster analysis showing poplar root primary metabolites (GC-MS/MS experiment) that were differentially abundant ($p < 0.05$) according to a multisample ANOVA test (**a**). Green, minimal abundance; red, maximal abundance. Volcano plots representing the NM-Control vs NM-Pb (**b**) and M-Control vs M-Pb (**c**) comparisons: each point represents a compound (LC-MS/MS experiment): red points – compounds that were more abundant in the corresponding Pb treatment, green points – compounds that were more abundant in the corresponding Control treatment. (For interpretation of the references to colour in this figure legend, the reader is referred to the Web version of this article.)

The acute stress response is strong and quick to allow the plant to survive, whereas chronically exposed plants must adjust and fine-tune their physiology to continuous stress conditions (Kovalchuk et al., 2007). Protein turnover processes consume energy, and disturbances in protein homeostasis lead to decreased plant cell viability and growth (Hasan et al., 2017; Li et al., 2017). A comparison of Pb-tolerant and Pb-sensitive plant genotypes shows that successful stress adaptation is linked to the minimization of protein turnover costs: a lower number of affected proteins but more effective stress response (Kovalchuk et al., 2004; Sairam et al., 2005; Kosová et al., 2015). The effectiveness of proteome adjustments in chronically stressed poplars may be reflected in their relatively stable metabolome. In contrast to acute Pb stress, during which numerous metabolites are usually dysregulated (e.g., Huang, et al., 2017), under chronic mild Pb stress, the proteome response is sufficient to provide overall metabolome and phenotype stability.

Moreover, compared with the roots experiencing acute HM stress, NM-Pb roots exhibited increased abundances of HSP80 and HSP90, which have been reported to have increased abundance in a relatively stable proteome of chronically HM-stressed poplars (Szuba and Lorenc-Plucińska, 2018) and have been linked to stress adaptation and reducing the influence of a destabilized environment (Queitsch et al., 2002; Wang et al., 2004). Decreased or unchanged protein turnover processes have been previously observed in plants exposed to prolonged chronic stress (Kosová et al., 2015; Zemleduch-Barylska and Lorenc-Plucińska, 2016; Szuba and Lorenc-Plucińska, 2018), where only the proteins required for metabolome stability were upregulated.

The low protein turnover level, which was probably associated with a small number of damaged proteins, was also a result of a low ROS level (radicals are major causes of protein damage) observed in Pb-treated poplar roots (Jalmi et al., 2018). This phenomenon was probably the result of a successful enzymatic anti-ROS response (Kosová et al., 2015; Xu et al., 2017; see the section above). Finally, decreased protein turnover and metabolome stability would result in a decreased intensity of intracellular transport (Kosová et al., 2015) and may be one reason for the decreased actin abundance, which is also a known target of low Pb stress (Fig. 5a; Pourrut et al., 2013; Horiunova et al., 2016).

4.2. Effect of P. involutus colonization on the poplar root response to Pb exposure

Although ECM are known to increase plant HM tolerance and are considered a plant defense mechanism against HM toxicity (Jentschke and Godbold, 2000; Szuba, 2015; Szuba et al., 2017; Zhang et al., 2017b), the omic adjustments in HM-stressed ectomycorrhizal plants are largely unknown. Decreased or unchanged biometric parameters of ectomycorrhizal plants have been relatively frequently reported (Szuba, 2015). Here, the use of the *Paxillus* isolate, which triggered decreases in the growth, nutrition and overall fitness of all M poplars, gives us a unique opportunity to analyze the changes in plant molecular Pb perception influenced mainly by fungal biofilters.

In M roots exposed to Pb, we observed molecular signals for the activation of similar processes to those detected in NM-Pb poplars (e.g., Pb sequestration, cytoskeletal modifications, H+-ATPase-14-3-3 interactions, stabilization of protein turnover in chronically exposed plants and metabolome stability; Kosová et al., 2015; Zemleduch-Barylska and Lorenc-Plucińska, 2016; Szuba and Lorenc-Plucińska, 2018; Pourrut et al., 2013; Horiunova et al., 2016; Li et al., 2016), but they were much less intense than those in NM roots.

We found no stress-related protein characterized by increased abundance in M-Pb roots compared with its abundance in M-Control roots. Additionally, the abundance of antiradical enzymes, whose expression was upregulated in NM roots exposed to Pb (catalases, peroxidases or cytoplasmic oxidoreductases; see above), was not increased in M-Pb roots compared to M-Control roots; there were also no differences in H_2O_2 abundance (no ROS burst).

Interestingly, we detected a strong decrease in H_2O_2 in all M plants compared to NM plants.

Although H_2O_2 is also a key molecule in ECM functioning, and decreases in H_2O_2 observed in M plants may play some unknown signaling role in ECM-triggered poplar growth regulation (Gafur et al., 2004), the decrease in ROS found in M roots may also contribute to the increased tolerance of ectomycorrhizal plants (Zhang et al., 2017b).

The less-intensive proteomic response together with the decline in stress symptoms detected in M-Pb roots suggested that fungal

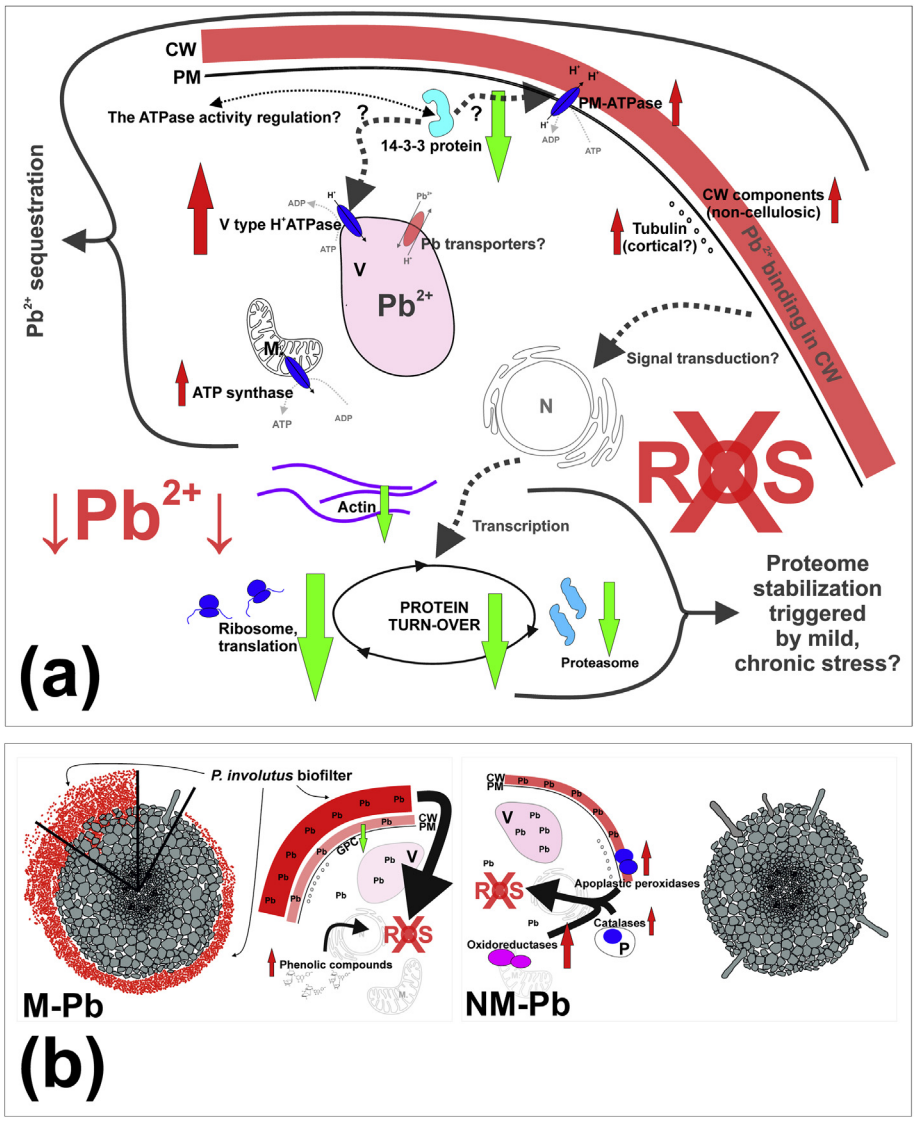

Fig. 5. Probable mechanisms of the plant root response to chronic mild Pb stress. Common root cell responses proposed for plant cells in NM and M poplar roots (**a;** for an explanation, see the main manuscript). Undetected but proposed mechanisms or interactions are marked with dotted lines. Differences in the response to Pb exposure between the NM and M treatments, showing the main players in the anti-Pb response (**b**). The *P. involutus* mantle is marked in red (fractions marked on the root cross-section correspond to the actual colonization level of M roots presented in Fig. 1c). CW – cell wall; M – mitochondrion; N – nucleus; P- peroxisome; PM – plasmalemma; V – vacuole. Red arrows – proteins with increased abundance in Pb treatments compared with Control treatments, green arrows – proteins with decreased abundance in Pb treatments. (For interpretation of the references to colour in this figure legend, the reader is referred to the Web version of this article.)

mantle-covered poplar cells were exposed to lower Pb concentrations than the 'bare' NM-Pb roots (Fig. 5b; confirmed by our mineral and microscopic experiments). There was no need for energy-consuming activation of the enzymatic machinery of the antioxidant response or protein restoration, probably because of the small number of Pb-damaged macromolecules in M-Pb plant cells. Moreover, ECM are also known to not only alleviate but also prevent stress symptoms, e.g., via stimulation of phenolic compounds, which are, among others, known antioxidants (Fig. 5b; Schützendübel and Polle, 2002; Michalak, 2006).

When stress levels exceed the toxicity threshold, regardless of the generally protective role of symbiosis, stress signals and strong defense responses are usually reported in stressed ectomycorrhizal plants (Ma et al., 2014; Luo et al., 2014). Moreover, enhanced HM uptake is frequently observed under ECM (Ma et al., 2014; Luo et al., 2014; Bojarczuk et al., 2015; Zhang et al., 2017b) and is considered to be positively related to the level of root colonization by ECM fungi (Jentschke and Godbold, 2000). We did not observe such an increase. The frequently reported stimulation of HM influx in ECM plants is usually linked to increases in HM transporter activity along with the necessary H+-ATPase activation (Ma et al., 2014; Luo et al., 2014; Zhang et al., 2017b; Shi et al., 2019). Concurrently, H+-ATPase activity under HM stress plays a vital role in the symport of citric acid (Zhang et al., 2017). Citric acid is one of the most important LMWOAs and is exported from HM-stressed ECM plants. Both protons and LMWOAs may decrease the ground medium pH (Shahid et al., 2012; Shi et al., 2019). In the present study, we observed an upregulation of H+-ATPases in M-Pb plants but (assumed) more acidic growth medium did not translate to increased Pb levels in M-Pb poplars, especially in aboveground tissues (compared with NM-Pb levels). Interestingly, LMWOAs are believed to increase Pb salt solubility by decreasing pH, but they have little effect on Pb translocation in plants (Shahid et al., 2012). This phenomenon could be caused by chelation of Pb in the

rhizosphere by more-abundant organic acid anions (Zhang et al., 2017). We did not detect differences in organic acids between M-Pb and M-Control treatments, but strong increases in enzymes involved in citrate biosynthesis (Zhang et al., 2017: malate dehydrogenase, phosphoenolpyruvate carboxylase and citrate synthase) and in citrate itself were detected in M roots compared with NM roots (the effect of poplar root colonization under Control conditions; Szuba, unpublished results).

LMWOAs are known players in Pb detoxification (Shi et al., 2019), but ECM roots also exclude numerous other compounds that are important for successful Pb chelation in the rhizosphere. Metallothionines, soluble proteins or phenolics (Vodnik et al., 1998; Jacob et al., 2004; Luo et al., 2014; Reddy et al., 2016) could be responsible for decreasing the concentrations (to μg mg $^{-1}$ dry weight) of lead in M-Pb roots. Moreover, phenolics (upregulated in M-Pb poplars) are transformed by laccases (upregulated in HM-stressed ECM; Jacob et al., 2004) into melanin, which may have been responsible for the dark pigmentation of the ground medium observed under ECM (Fig. S1) and represent another known Pb chelator (Cordero et al., 2017).

Altogether, our results strongly suggest that the protective fungal hyphae, i.e., the *P. involutus* biofilter, decreased the amounts of Pb affecting poplar cells (Fig. 5b; Marschner et al., 1998; Colpaert et al., 2011; Luo et al., 2014; Shi et al., 2019). The increases in M-Pb poplar mass compared with M-Control mass suggest that ECM alleviate Pb effects in plants (Schützendübel and Polle, 2002; Ma et al., 2014) and that Pb in the plant cytosol has a concentration range that triggers a hormesis effect (reported previously for plants exposed to a low Pb dose; Wang et al., 2010; Szuba et al., 2017). Root colonization by ectomycorrhizal fungi is unambiguously beneficial for HM-stressed plants.

Funding

This work was funded by the National Science Center, Poland (DEC-2011/03/D/NZ9/05500) and was supported by the Institute of Dendrology Polish Academy of Sciences (PAS), the Institute of Bioorganic Chemistry PAS and by Jan Kochanowski University, Poland.

Author contribution statement

AS designed and conducted all experiments, analyzed the data and wrote the manuscript. ŁM conducted mass spectrometry experiments, analyzed the MS/MS data and edited the manuscript. RK conducted mineral experiments and edited the manuscript.

Declaration of competing interest

The authors declare that they have no known competing financial interests or personal relationships that could have appeared to influence the work reported in this paper.

CRediT authorship contribution statement

Agnieszka Szuba: Conceptualization, Methodology, Validation, Formal analysis, Investigation, Resources, Writing - original draft, Writing - review & editing, Visualization, Supervision, Project administration, Funding acquisition. **Łukasz Marczak:** Methodology, Validation, Formal analysis, Investigation, Data curation, Writing - review & editing. **Rafał Kozłowski:** Methodology, Validation, Investigation, Data curation, Writing - review & editing.

Acknowledgments

The authors thank Prof. G. Lorenc-Plucińska, Prof. M. Rudawska, Prof. T. Leski, Dr. L. Karliński and Prof. J. Mucha from the Institute of Dendrology for their valuable assistance and discussions. We thank the editors and the reviewers who provided helpful advice to improve this paper.

Appendix A. Supplementary data

Supplementary data to this article can be found online at https://doi.org/10.1016/j.envpol.2020.114585.

References

Babst, M., 2014. Quality control at the plasma membrane: one mechanism does not fit all. J. Cell Biol. 205, 11–20. https://doi.org/10.1083/jcb.201310113.

Bojarczuk, K., Karliński, L., Hazubska-Przybył, T., Kieliszewska-Rokicka, B., 2015. Influence of mycorrhizal inoculation on growth of micropropagated *Populus* × *canescens* lines in metal-contaminated soils. N. For. 46, 195–215. https://doi.org/10.1007/s11056-014-9455-3.

Chen, Q., Kan, Q., Wang, P., Yu, W., Yu, Y., Zhao, Y., Yu, Y., Li, K., Chen, L., 2015. Phosphorylation and interaction with the 14-3-3 protein of the plasma membrane H+-ATPase are involved in the regulation of magnesium-mediated increases in aluminum-induced citrate exudation in broad bean (*Vicia faba*. L). Plant Cell Physiol. 56, 1144–1153. https://doi.org/10.1093/pcp/pcv038.

Colpaert, J.V., Wevers, J.H.L., Krznaric, E., Adriaensen, K., 2011. How metal-tolerant ecotypes of ectomycorrhizal fungi protect plants from heavy metal pollution. Ann. For. Sci. 68, 17–24. https://doi.org/10.1007/s13595-010-0003-9.

Cordero, R.J.B., Vij, R., Casadevall, A., 2017. Microbial melanins for radioprotection and bioremediation. Microb. Biotechnol. 10, 1186–1190. https://doi.org/10.1111/1751-7915.12807.

Éva, C., Zelenyánszki, H., Tömösközi-Farkas, R., Tamás, L., 2014. Overproduction of an Arabidopsis aldo–keto reductase increases barley tolerance to oxidative and cadmium stress by an in vivo reactive aldehyde detoxification. Plant Growth Regul. 74, 55–63. https://doi.org/10.1016/j.sajb.2014.04.010.

Fahr, M., Laplaze, L., Bendaou, N., Hocher, V., Mzibri, M.E., Bogusz, D., Smouni, A., 2013. Effect of lead on root growth. Front. Plant Sci. 4, 175. https://doi.org/10.3389/fpls.2013.00175.

Gafur, A., Schützendübel, A., Langenfeld–Heyser, R., Fritz, E., Polle, A., 2004. Compatible and incompetent *Paxillus involutus* isolates for ectomycorrhiza formation in vitro with poplar (*Populus x canescens*) differ in H_2O_2 production. Plant Biol. (Stuttg) 6, 91–99. https://doi.org/10.1055/s-2003-44718.

Hasan, M.K., Cheng, Y., Kanwar, M.K., Chu, X.-Y., Ahammed, G.J., Qi, Z.-Y., 2017. Responses of plant proteins to heavy metal stress—a review. Front. Plant Sci. 8, 1492. https://doi.org/10.3389/fpls.2017.01492.

Horiunova, I.I., Krasylenko, Y.A., Yemets, A.I., Blume, Y.B., 2016. Involvement of plant cytoskeleton in cellular mechanisms of metal toxicity. Cytol. Genet. 50, 57–67. https://doi.org/10.3103/S0095452716010060.

Huang, X., Lei Wang, L., Laserna, A.K.C., Li, S.F.Y., 2017. Correlations in the elemental and metabolic profiles of the lichen *Dirinaria picta* after road traffic exposure. Metallomics 9, 1610–1621. https://doi.org/10.1039/c7mt00207f.

Jacob, C., Courbot, M., Martin, F., Brun, A., Chalot, M., 2004. Transcriptomic responses to cadmium in the ectomycorrhizal fungus *Paxillus involutus*. FEBS Lett. 576, 423–427. https://doi.org/10.1016/j.febslet.2004.09.028.

Jalmi, S.K., Bhagat, P.K., Verma, D., Noryang, S., Tayyeba, S., Singh, K., Sharma, D., Sinha, A.K., 2018. Traversing the links between heavy metal stress and plant signaling. Front. Plant Sci. 9, 12. https://doi.org/10.3389/fpls.2018.00012.

Jentschke, G., Godbold, D.L., 2000. Metal toxicity and ectomycorrhizas. Physiol. Plantarum 109, 107–116. https://doi.org/10.1034/j.1399-3054.2000.100201.x.

Jiang, D., Wang, Y., Dong, X., Yan, S., 2018. Inducible defense responses in *Populus alba* berolinensis to Pb stress. South Afr. J. Bot. 119, 295–300. https://doi.org/10.1016/j.sajb.2018.09.030.

Johansson, E.M., Fransson, P.A.M., Finlay, R.D., van Hees, P.A.V., 2008. Quantitative analysis of root and ectomycorrhizal exudates as a response to Pb, Cd and as stress. Plant Soil 313, 39–54. https://doi.org/10.1007/s11104-008-9678-1.

Kirankumar, T.V., Madhusudhan, K.V., Nareshkumar, A., Kiranmai, K., Lokesh, U., Venkatesh, B., Sudhakar, Ch, 2016. Expression analysis of aldo-keto reductase 1 (AKR1) in foxtail millet (*Setaria italica* L.) subjected to abiotic stresses. Am. J. Plant Sci. 7, 500–509. https://doi.org/10.4236/ajps.2016.73044.

Klychnikov, O.I., Li, K.W., Lill, H., de Boer, A.H., 2007. The V-ATPase from etiolated barley (*Hordeum vulgare* L.) shoots is activated by blue light and interacts with 14-3-3 proteins. J. Exp. Bot. 58, 1013–1023. https://doi.org/10.1093/jxb/erl261.

Kopittke, P.M., Asher, C.J., Menzies, N.W., 2008. Prediction of Pb speciation in concentrated and dilute nutrient solutions. Environ. Pollut. 153, 548–554. https://doi.org/10.1016/j.envpol.2007.09.012.

Kosová, K., Vítámvás, P., Urban, M.O., Klíma, M., Roy, A., Prášil, I.T., 2015. Biological networks underlying abiotic stress tolerance in temperate crops—a proteomic perspective. Int. J. Mol. Sci. 16, 20913–20942. https://doi.org/10.3390/ijms160920913.

Kovalchuk, Igor, Abramov, Vladimir, Pogribny, Igor, Kovalchuk, Olga, 2004. Adaptation to Life in the Chernobyl Zone. Plant Physiol. 135 (1), 357–363. https://doi.org/10.1104/pp.104.040477.

Kovalchuk, I., Molinier, J., Yao, Y., Arkhipov, A., Kovalchuk, O., 2007. Transcriptome analysis reveals fundamental differences in plant response to acute and chronic exposure to ionizing radiation. Mutat. Res. 624, 101–113. https://doi.org/10.1016/j.mrfmmm.2007.04.009.

Krzesłowska, M., 2011. The cell wall in plant cell response to trace metals: polysaccharide remodeling and role in defense strategy. Acta Physiol. Plant. 33, 35–51. https://doi.org/10.1007/s11738-010-0581-z.

Li, G.K., Gao, J., Peng, H., Shen, Y.O., Ding, H.P., Zhang, Z.M., Pan, G.T., Lin, H.J., 2016. Proteomic changes in maize as a response to heavy metal (lead) stress revealed by iTRAQ quantitative proteomics. Genet. Mol. Res. 15 (1) https://doi.org/10.4238/gmr.15017254.

Li, L., Nelson, C.J., Trösch, J., Castleden, I., Huang, S., Millar, A.H., 2017. Protein degradation rate in *Arabidopsis thaliana* leaf growth and development. Plant Cell 29, 207–228. https://doi.org/10.1105/tpc.16.00768.

Liu, H., Zhao, H., Wu, L., Liu, A., Zhao, F.J., Xu, W., 2017. Heavy metal ATPase 3 (HMA3) confers cadmium hypertolerance on the cadmium/zinc hyperaccumulator *Sedum plumbizincicola*. New Phytol. 215, 687–698. https://doi.org/10.1111/nph.14622.

Luo, Z.-B., Wu, Ch, Zhang, Ch, Li, H., Lipka, U., Polle, A., 2014. The role of ectomycorrhizas in heavy metal stress tolerance of host plants. Environ. Exp. Bot. 108, 47–62. https://doi.org/10.1016/j.envexpbot.2013.10.018.

Ma, Y., He, J., Ma, C., Luo, J., Li, H., Liu, T., Polle, A., Peng, C., Luo, Z.B., 2014. Ectomycorrhizas with *Paxillus involutus* enhance cadmium uptake and tolerance in *Populus* × *canescens*. Plant Cell Environ. 37, 627–642. https://doi.org/10.1111/pce.12183.

Marschner, P., Jentschke, G., Godbold, D., 1998. Cation exchange capacity and lead sorption in ectomycorrhizal fungi. Plant Soil 205, 93–98. https://doi.org/10.1023/A:1004376727051.

Michalak, A., 2006. Phenolic compounds and their antioxidant activity in plants growing under heavy metal stress. Pol. J. Environ. Stud. 15, 523–530.

Moin, M., Bakshi, A., Madhav, M.S., Kirti, P.B., 2017. Expression profiling of ribosomal protein gene family in dehydration stress responses and characterization of transgenic rice plants overexpressing RPL23A for water-use efficiency and tolerance to drought and salt stresses. Front. Chem. 5, 97. https://doi.org/10.3389/fchem.2017.00097.

Pourrut, B., Shahid, M., Douay, F., Dumat, C., Pinelli, E., 2013. Molecular mechanisms involved in lead uptake, toxicity and detoxification in higher plants. In: Gupta, D.K., et al. (Eds.), Heavy Metal Stress in Plants. Springer-Verlag Berlin Heidelberg. https://doi.org/10.1007/978-3-642-38469-1_7.

Queitsch, C., Sangster, T.A., Lindquist, S., 2002. Hsp90 as a capacitor of phenotypic variation. Nature 417, 618–624. https://doi.org/10.1038/nature749.

Reddy, M.S., Kour, M., Aggarwal, S., Ahuja, S., Marmeisse, R., Fraissinet-Tachet, L., 2016. Metal induction of a *Pisolithus albus* metallothionein and its potential involvement in heavy metal tolerance during mycorrhizal symbiosis. Environ. Microbiol. 18 https://doi.org/10.1111/1462-2920.13149, 2446–54.

Sairam, R.K., Srivastava, G.C., Agarwal, S., Meena, R.C., 2005. Differences in antioxidant activity in response to salinity stress in tolerant and susceptible wheat genotypes. Biol. Plant. (Prague) 49, 85–91. https://doi.org/10.1007/s10535-005-5091-2.

Schützendübel, A., Polle, A., 2002. Plant responses to abiotic stresses: heavy metal-induced oxidative stress and protection by mycorrhization. J. Exp. Bot. 53, 1351–1365. https://doi.org/10.1093/jexbot/53.372.1351.

Shahid, M., Pinelli, E., Dumat, C., 2012. Review of Pb availability and toxicity to plants in relation with metal speciation; role of synthetic and natural organic ligands. J. Hazard Mater. 219–220, 1–12. https://doi.org/10.1016/j.jhazmat.2012.01.060.

Sharma, S.S., Dietz, K.-J., Mimura, T., 2016. Vacuolar compartmentalization as indispensable component of heavy metal detoxification in plants. Plant Cell Environ. 39, 1112–1126. https://doi.org/10.1111/pce.12706.

Shen, Y., Zhang, Y., Chen, J., Lin, H., Zhao, M., Peng, H., Liu, L., Yuan, G., Zhang, S., Zhang, Z., Pan, G., 2013. Genome expression profile analysis reveals important transcripts in maize roots responding to the stress of heavy metal Pb. Physiol. Plant. 147, 270–282. https://doi.org/10.1111/j.1399-3054.2012.01670.x.

Shi, W., Zhang, Y., Chen, S., Polle, A., Rennenberg, H., Luo, Z.-B., 2019. Physiological and molecular mechanisms of heavy metal accumulation in nonmycorrhizal versus mycorrhizal plants. Plant Cell Environ. 42, 1087–1103. https://doi.org/10.1111/pce.13471.

Smith, S.E., Read, D., 2008. Mycorrhizal Symbiosis. Academic Press, London, UK.

Swarcewicz, B., Sawikowska, A., Ł, Marczak, Łuczak, M., Ciesiołka, D., Krystkowiak, K., Kuczyńska, A., Piślewska-Bednarek, M., Krajewski, P., Stobiecki, M., 2017. Effect of drought stress on metabolite contents in barley recombinant inbred line population revealed by untargeted GC–MS profiling. Acta Physiol. Plant. 39, 158. https://doi.org/10.1007/s11738-017-2449-y.

Szuba, A., 2015. Ectomycorrhiza of populus. For. Ecol. Manag. 347, 156–169. https://doi.org/10.1016/j.foreco.2015.03.012.

Szuba, A., Karliński, L., Krzesłowska, M., Hazubska–Przybył, T., 2017. Inoculation with a Pb–tolerant strain of *Paxillus involutus* improves growth and Pb tolerance of *Populus* × *canescens* under in vitro conditions. Plant Soil 412, 253–266. https://doi.org/10.1007/s11104-016-3062-3.

Szuba, A., Lorenc-Plucińska, G., 2018. Field proteomics of *Populus alba* grown in a heavily modified environment – an example of a tannery waste landfill. Sci. Total Environ. 610, 1557–1571. https://doi.org/10.1016/j.scitotenv.2017.06.102.

Szuba, A., Ł, Marczak, Karliński, L., Mucha, J., Tomaszewski, D., 2019. Regulation of the leaf proteome by inoculation of *Populus* ×*canescens* with two *Paxillus involutus* isolates differing in root colonization rates. Mycorrhiza 29, 503–517. https://doi.org/10.1007/s00572-019-00910-5.

Szuba, A., Wojakowska, A., Lorenc-Plucińska, G., 2013. An optimized method to extract poplar leaf proteins for two-dimensional gel electrophoresis guided by analysis of polysaccharides and phenolic compounds. Electrophoresis 34, 3234–3243. https://doi.org/10.1002/elps.201300223.

Tang, Y., Shi, L., Zhong, K., Shen, Z., Chen, Y., 2019. Ectomycorrhizal fungi may not act as a barrier inhibiting host plant absorption of heavy metals. Chemosphere 215, 115–123. https://doi.org/10.1016/j.chemosphere.2018.09.143.

Tangahu, B.V., Abdullah, S.R.S., Basri, H., Idris, M., Anuar, N., Mukhlisin, M., 2011. A review on heavy metals (as, Pb, and Hg) uptake by plants through phytoremediation. Int. J. Chem. Eng. 939161, 1–30. https://doi.org/10.1155/2011/939161.

Vemanna, R.S., Babitha, K.C., Solanki, J.K., Amarnatha Reddy, V., Sarangi, S.K., Udayakumar, M., 2017. Aldo-keto reductase-1 (AKR1) protect cellular enzymes from salt stress by detoxifying reactive cytotoxic compounds. Plant Physiol. Bioch. 113, 177–186. https://doi.org/10.1016/j.plaphy.2017.02.012.

Visioli, G., Vincenzi, S., Marmiroli, M., Marmiroli, N., 2012. Correlation between phenotype and proteome in the Ni hyperaccumulator *Noccaea caerulescens subsp*. Caerulescens. Environ. Exp. Bot. 77, 156–164. https://doi.org/10.1016/j.envexpbot.2011.11.016.

Vodnik, D., Byrne, A.R., Gogala, N., 1998. The uptake and transport of lead in some ectomycorrhizal fungi in culture. Mycol. Res. 102, 953–958. https://doi.org/10.1017/S0953756297005959.

Wang, Ch-R., Tian, Y., Wang, X.-R., Yu, H.-X., Lu, X.-W., Wang, Ch, Wang, H., 2010. Hormesis effects and implicative application in assessment of lead-contaminated soils in roots of *Vicia faba* seedlings. Chemosphere 80, 965–971. https://doi.org/10.1016/j.chemosphere.2010.05.049.

Wang, W., Vinocur, B., Shoseyov, O., Altman, A., 2004. Role of plant heat-shock proteins and molecular chaperones in the abiotic stress response. Trends Plant Sci. 9, 244–252. https://doi.org/10.1016/j.tplants.2004.03.006.

Wang, X.H., Wang, Q., Nie, Z.W., He, L.Y., Sheng, X.F., 2018. *Ralstonia eutropha* Q2-8 reduces wheat plant above-ground tissue cadmium and arsenic uptake and increases the expression of the plant root cell wall organization and biosynthesis-related proteins. Environ. Pollut. 242, 1488–1499. https://doi.org/10.1016/j.envpol.2018.08.039.

Wang, Y., Xu, L., Chen, Y., Shen, H., Gong, Y., et al., 2013. Transcriptome profiling of radish (*Raphanus sativus* L.) root and identification of genes involved in response to lead (Pb) stress with next generation sequencing. PloS One 8 (6), e66539. https://doi.org/10.1371/journal.pone.0066539.

Wang, Y., Xu, L., Tang, M., Jiang, H., Chen, W., Zhang, W., Wang, R., Liu, L., 2016. Functional and Integrative analysis of the proteomic profile of radish root under Pb exposure. Front. Plant Sci. 7, 1871. https://doi.org/10.3389/fpls.2016.01871.

Wang, Y.-H., Garvin, D.F., Kochian, L.V., 2002. Rapid induction of regulatory and transporter genes in response to phosphorus, potassium, and iron deficiencies in tomato roots. Evidence for cross talk and root/rhizosphere-mediated signals. Plant Physiol. 130, 1361–1370. https://doi.org/10.1104/pp.008854.

Williams, L.E., Pittman, J.K., Hall, J.L., 2000. Emerging mechanisms for heavy metal transport in plants. Biochim. Biophys. Acta 1465, 104–126. https://doi.org/10.1016/s0005-2736(00)00133-4.

Xie, C., Hu, L., Yang, Y., Liao, D., Yang, X., 2017. Accumulation and tolerance to cadmium heavy metal ions and induction of 14-3-3 gene expression in response to cadmium exposure in *Coprinus atramentarius*. Microbiol. Res. 196, 1–6. https://doi.org/10.1016/j.micres.2016.11.012.

Xu, B., Wang, Y., Zhang, S., Guo, Q., Jin, Y., Chen, J., et al., 2017. Transcriptomic and physiological analyses of Medicago sativa L. roots in response to lead stress. PloS One 12 (4), e0175307. https://doi.org/10.1371/journal.pone.0175307.

Yamaji, K., Watanabe, Y., Masuya, H., Shigeto, A., Yui, H., Haruma, T., 2016. Root Fungal endophytes enhance heavy-metal stress tolerance of *Clethra barbinervis* growing naturally at mining sites via growth enhancement, promotion of nutrient uptake and decrease of heavy-metal concentration. PloS One 11 (12), e0169089. https://doi.org/10.1371/journal.pone.0169089.

Zemleduch-Barylska, A., Lorenc-Plucińska, G., 2016. Response of leaf and fine roots proteomes of *Salix viminalis* L. to growth on Cr-rich tannery waste. Environ. Sci. Pollut. Res. 23, 18394–18406. https://doi.org/10.1007/s11356-016-7026-1.

Zhang, J., Wei, J., Li, D., Kong, X., Rengel, Z., Chen, L., Yang, Y., Cui, X., Chen, Q., 2017. The role of the plasma membrane H+-ATPase in plant responses to aluminum toxicity. Front. Plant Sci. 8, 1757. https://doi.org/10.3389/fpls.2017.01757.

Zhang, Y., Ge, F., Hou, F., Sun, W., Zheng, Q., Zhang, X., Ma, L., Fu, J., He, X., Peng, H., Pan, G., Shen, Y., 2017a. Transcription factors responding to Pb stress in maize. Genes 8, 231. https://doi.org/10.3390/genes8090231.

Zhang, Y., Sa, G., Zhang, Y., Zhu, Z., Deng, S., Sun, J., Li, N., Li, J., Yao, J., Zhao, N., Zhao, R., Ma, X., Polle, A., Chen, S., 2017b. *Paxillus involutus*-facilitated Cd_2C influx through plasma membrane Ca_2C-permeable channels is stimulated by H_2O_2 and HC-ATPase in ectomycorrhizal *Populus* × *canescens* under cadmium stress. Front. Plant Sci. 7, 1975. https://doi.org/10.3389/fpls.